



Revisiting the symmetric reactions for synthesis of super-heavy nuclei of $Z \geq 120$



R.K. Choudhury¹, Y.K. Gupta*

Nuclear Physics Division, Bhabha Atomic Research Centre, Trombay, Mumbai 400085, India

ARTICLE INFO

Article history:

Received 29 December 2013
 Received in revised form 9 February 2014
 Accepted 14 February 2014
 Available online 20 February 2014
 Editor: V. Metag

Keywords:

Super-heavy elements
 Symmetric reactions
 Rare-earth nuclei
 Fusion by Diffusion model

ABSTRACT

Extensive efforts have been made experimentally to reach nuclei in the super-heavy mass region of $Z = 110$ and above with suitable choices of projectile and target nuclei. The cross sections for production of these nuclei are seen to be in the range of a few picobarn or less, and pose great experimental challenges. Theoretically, there have been extensive calculations for highly asymmetric (hot-fusion) and moderately asymmetric (cold-fusion) collisions and only a few theoretical studies are available for near-symmetric collisions to estimate the cross sections for production of super-heavy nuclei. In the present article, we revisit the symmetric heavy ion reactions with suitable combinations of projectile and target nuclei in the rare-earth region, that will lead to super-heavy nuclei of $Z \geq 120$ with measurable fusion cross sections.

© 2014 The Authors. Published by Elsevier B.V. Open access under CC BY license. Funded by SCOAP³.

1. Introduction

An island of super-heavy nuclei, with half-lives ranging from a few seconds to a few thousands of years, has been predicted by calculations based on macroscopic–microscopic theories [1–5]. The large stability arises due to strong shell effects in the range of proton numbers ($Z = 114$ – 126) and neutron numbers ($N = 170$ – 188), which in turn gives rise to large fission barriers (5–8 MeV) in this mass region. There have been extensive efforts experimentally to synthesize super-heavy elements (SHE) through heavy ion reactions with suitable choice of projectile and target nuclei. However, the compound nuclei are formed in the excitation energy of few tens of MeV, and due to washing out of shell effects with increasing excitation energy, the production cross sections are usually quite low (in the range of picobarns or less) for compound nuclei with $Z = 110$ and above. Nevertheless, nuclei with Z up to 118 so far have been synthesized in laboratory by various experiments [6–16].

Theoretically, there have been many attempts to understand the reaction mechanism leading to the formation of the super-heavy nuclei [17–23]. Based upon the various theoretical formalisms, different reaction routes for the synthesis of super-heavy nuclei have

been proposed [24–29]. The main considerations in selecting a reaction channel for producing super-heavy nuclei are the following:

1. Large fusion cross section.
2. Larger fusion $|Q|$ -value over the Coulomb barrier (V_{Coul}) for low excitation energy of CN, giving rise to optimum survival probability.
3. Proper neutron-to-proton ratio (n/p) of CN for better stability.
4. High beam intensity and target concentration for good yield.

The two main routes followed are: ‘hot fusion’ with actinide target nuclei and highly asymmetric reaction channels [6–12], and ‘cold fusion’ with Pb, Bi target nuclei with moderately asymmetric reaction channels [13–16]. As mentioned above, the cross sections for SHE production have been found to be in the range of only a few picobarn or less in the experiments carried out so far. Recent reviews [20,30–32] have emphasized on radioactive-ion-beam routes for producing $Z_{\text{CN}} \geq 120$. In order to have better survival probability, radioactive neutron rich beams (^{96}Sr , ^{132}Sn) are being suggested to reach a more suitable neutron/proton combination. However, these reactions will have severe limitation on beam intensity.

2. Symmetric heavy-ion collisions using rare-earth nuclei

There have been some attempts using nearly symmetric collisions such as $^{136}\text{Xe} + ^{136}\text{Xe}$ to synthesize Hs nuclei for which upper limit of the production cross section was obtained to be

* Corresponding author.

E-mail addresses: rkc.slr@gmail.com (R.K. Choudhury), ykg.barc@gmail.com (Y.K. Gupta).

¹ Ex-BARC, Mumbai, India.

Table 1

Relevant data for the new reaction routes using the rare-earth nuclei.

Reaction (Z_{CN} , A_{CN})	$Z_P Z_T$	g.s. deformations (Projectile, Target)	Q -value (MeV)	V_{Coul} (MeV)	S_n (MeV)
$^{154}\text{Sm} + ^{150}\text{Nd}$ (122, 304)	3720	(0.27, 0.24)	−377.5	373.9	7.1
$^{154}\text{Sm} + ^{154}\text{Sm}$ (124, 308)	3844	(0.27, 0.27)	−394.9	385.5	7.1
$^{160}\text{Gd} + ^{154}\text{Sm}$ (126, 314)	3968	(0.28, 0.27)	−412.2	396.2	7.3

4 picobarns [33]. The symmetric collisions using deformed projectile and target nuclei have also been suggested earlier [26–28] to synthesize super-heavy nuclei. For $^{149}\text{La} + ^{149}\text{La}$ collision to produce $Z = 114$ nuclei, the upper limit of cross section was estimated from theoretical consideration to be around 10 picobarns [29]. However, there is no experimental data available for this system. In the following, we revisit the near-symmetric collisions involving rare-earth nuclei that might prove useful for synthesis of cold super-heavy nuclei.

Table 1 shows some relevant data such as the $Z_P Z_T$ value, ground state (g.s.) deformations of projectile and target nuclei (from Ref. [34]), the fusion Q -value, V_{Coul} and the neutron separation energy (S_n) for certain reaction routes using rare-earth nuclei fusion channels. The Q and S_n values are calculated using the predicted masses by Möller and Nix [34]. The V_{Coul} values are taken from the NRV code [35] which are consistent with the parameterizations of mean value of the barrier distribution given in Ref. [21]. In addition to the reactions shown in Table 1, many more fusion reaction channels are feasible using other different rare-earth target/projectile combinations. The advantages that these reactions offer are:

1. $V_{Coul} < |Q|$ value.
2. Large g.s. deformations of both target and projectile nuclei that might enhance near-barrier fusion cross section by channel coupling and lowering of fusion barrier, B_{fus} .
3. Good n/p ratio of CN.
4. Stable beams for large beam intensity.
5. Large elemental abundances of rare-earth elements.
6. Large center-of-mass velocity for better collection of CN residues in forward direction.
7. Low neutron background at optimum low bombarding energy.

For example, in case of $^{160}\text{Gd} + ^{154}\text{Sm}$ reaction, the CN is (126, 314) where V_{Coul} is 16 MeV lower than the energy required ($|Q|$ -value) for initiating the reaction. With optimum bombarding energy above the Coulomb barrier, the CN can be produced with relatively low excitation energy.

3. Theoretical estimates

We will now describe the method adopted in this work to calculate the fusion/survival probability of the above rare-earth reaction channels. One expects that due to large $Z_P Z_T$ product, fusion will be largely hindered. However, for deformed nuclei there is no clear cut understanding of the fusion hindrance (except the extra-push effects suggested by W. Swiatecki [36,37]). There are calculations reported in literature, where only target deformation is considered [22]. We discuss below the basic method to estimate the SHE formation cross section using rare-earth nuclear collisions.

In case of heavy colliding systems typically used for super-heavy mass-region, overcoming the Coulomb barrier is not enough to form the super-heavy compound nucleus. There are two avenues for estimating the compound nuclear formation cross section for

heavy colliding nuclei similar to the ones discussed in the present article. These are: (i) extra-extra-push model [36,37] and (ii) Fusion by Diffusion model (FBD) [18]. According to the extra-extra-push model, an extra-energy ('extra-extra-push') with respect to the Coulomb barrier is needed to land inside the unconditional saddle point which guards the colliding system against re-separation before forming the compound nucleus. The 'extra-extra-push' energy increases rapidly with effective fissility [37]. For the present reactions where deformed projectile and target nuclei are considered, due to broad Coulomb barrier distribution, a large amount of 'extra-extra-push' energy could be available (~ 100 MeV) at very low probability for certain orientations of the colliding deformed nuclei. However, the entrance channel barrier distributions for these kind of heavy deformed nuclei with inclusion of dynamical effects are not easily calculable.

On the other hand, the FBD model has been successfully employed in reproducing the measured excitation function of the super-heavy element synthesis [18]. A set of twelve fusion reactions has been analyzed with the original version of the FBD model by Swiatecki et al. [18]. In another work, experimental excitation functions of a complete set of 27 cold fusion reactions have been reproduced using the FBD model by Cap et al. [21]. In the FBD model, the evaporation residue cross section σ_{ER} for production of a given final nucleus in its ground state is factorized as the product of the partial sticking cross section σ_{stick} , the diffusion probability P_{Diffus} , and the survival probability P_{surv} [17,21]:

$$\sigma_{ER}(E_{c.m.}) = \sigma_{stick}(E_{c.m.})P_{Diffus}(E_{c.m.})P_{surv}(E_{c.m.}) \quad (1)$$

$$= \frac{\pi \hbar^2}{2\mu E_{c.m.}} \sum_{\ell=0}^{\ell_{max}} (2\ell + 1) P_{Diffus}(E_{c.m.}) P_{surv}(E_{c.m.}). \quad (2)$$

By replacing the summation in above equation by an integral, one obtains the sticking cross section as:

$$\sigma_{stick}(E_{c.m.}) = \frac{\pi \hbar^2}{2\mu E_{c.m.}} (\ell_{max} + 1)^2, \quad (3)$$

where ℓ_{max} is the maximum angular momentum and it is determined by the "diffused barrier formula" based on assumption of Gaussian distribution of the barriers around a mean value B_0 (see Ref. [21] for details). The sticking cross sections determined for the present reactions are shown in Fig. 1(a) as a function of $Z_P Z_T$ at two center-of-mass energies: (i) $E_{c.m.} = V_{Coul}$ and (ii) $E_{c.m.}$ values for which initial excitation energy of the CN, $E_X = 10$ MeV. Corresponding center-of-mass energies as a function of $Z_P Z_T$ are shown in Fig. 1(b). The difference between the $E_{c.m.}$ values for $E_{c.m.} = V_{Coul}$ and $E_X = 10$ MeV increases with $Z_P Z_T$ which is reflected in the behavior of sticking cross section as a function of $Z_P Z_T$. The lines in Fig. 1(a) and (b) are shown to guide the eye.

Here, we are using original version of the FBD model [17], where angular momentum dependence of the diffusion and survival probabilities are not taken into account. The probability (P_{Diffus}) that the system injected at a point outside the saddle

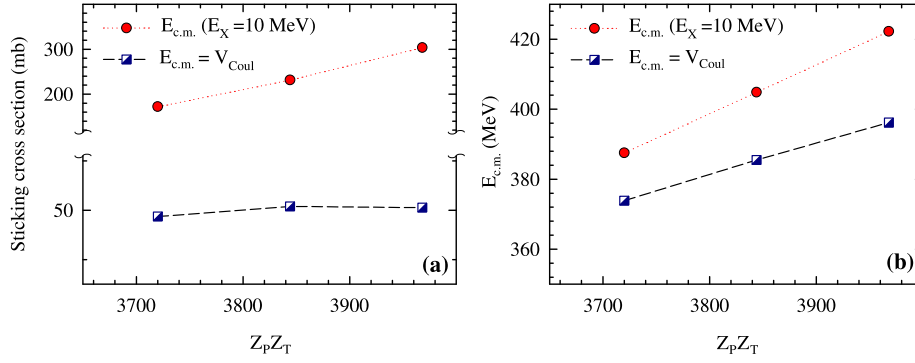


Fig. 1. (Color online.) (a) Sticking cross section at two different $E_{c.m.}$ values as a function of $Z_p Z_T$ for the reactions discussed in the present work. Solid circles are for $E_{c.m.}$ values for which $E_X = 10 \text{ MeV}$ and squares are for $E_{c.m.} = V_{Coul}$, corresponding center-of-mass energies as a function of $Z_p Z_T$ in (b). The lines in (a) and (b) are shown to guide the eye.

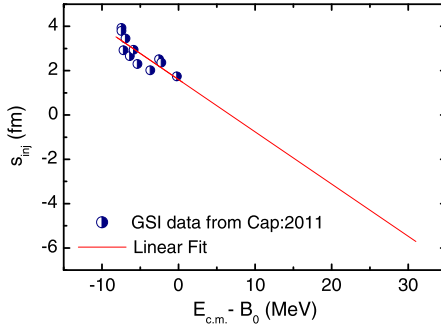


Fig. 2. The injection parameter (s_{inj}) as a function of $(E_{c.m.} - B_0)$ taken from Ref. [21]. The solid line is the least square linear fit, $s_{inj} = 1.5985 - 0.23587(E_{c.m.} - B_0) \text{ fm/MeV}$.

point achieves fusion is calculated using the diffusion process over a parabolic barrier [18]. If L stands for the total length of di-nuclear shape, the parameter s is defined as $s = L - 2(R_1 + R_2)$. In the entrance channel of two approaching nuclei, $s = 0$ would correspond to contact of half-density contours. The diffusion probability P_{Diffus} is then given by [18,21]:

$$P_{Diffus} = \frac{1}{2}(1 - \text{erf}\sqrt{H/T}), \quad (4)$$

where H is barrier height opposing fusion along the asymmetric fission valley, as seen from the injection point (s_{inj}). T is the temperature of the fusing system, which decreases during the uphill diffusion from an initial temperature at the injection point T_{inj} to a lower value at the saddle point T_{saddle} . In Eq. (4), mean of these two values has been used. The diffusion probability decreases very rapidly (depending on T) with increasing barrier height H . At a given H , P_{Diffus} is larger for a higher temperature value.

The macroscopic deformation energies are calculated as a function of the parameter s using the improved version of algebraic equations [21]. In order to estimate the barrier height, H , s_{inj} is a crucial parameter. In the FBD model, s_{inj} is a free parameter which is adjusted to reproduce the measured fusion cross section. In the work by Cap et al. [21], s_{inj} has been deduced for 27 cold fusion reactions including GSI, LBNL and RIKEN data. In that work, the s_{inj} values are plotted as a function of the excess of kinetic energy above the Coulomb barrier, $(E_{c.m.} - B_0)$, where B_0 is the mean value of the Coulomb barrier (V_{Coul}). The overall trend of s_{inj} is of decreasing nature with increasing $(E_{c.m.} - B_0)$. It is seen from Ref. [21] that except for the GSI data, all other data are scattered. For the purpose of present reactions, s_{inj} values for GSI data are considered and a linear least-square fit is obtained as shown in Fig. 2, given by:

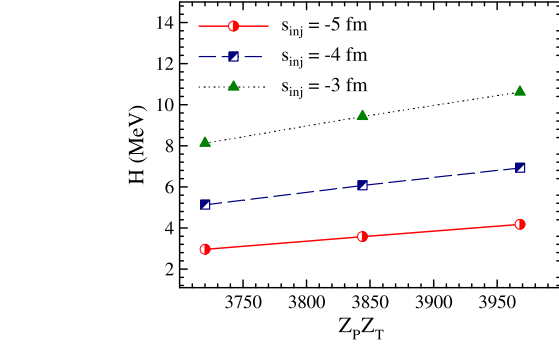


Fig. 3. (Color online.) The barrier height (H) as a function of $Z_p Z_T$ of the present reactions at various values of injection parameter (s_{inj}).

$$s_{inj} = 1.5985 - 0.23587(E_{c.m.} - B_0) \text{ fm/MeV}. \quad (5)$$

Since the present projectile and target nuclei are deformed ones, the fusion barrier distribution is expected to be quite broad [38]. Even at $E_X < 8 \text{ MeV}$, a large fraction of the barrier distribution will have $(E_{c.m.} - B_0) > 30 \text{ MeV}$, which will lead to $s_{inj} \sim -5 \text{ fm}$ as reflected from Fig. 2. For the present reactions, the barrier height, H is calculated at $s_{inj} = -5, -4,$ and -3 fm as shown in Fig. 3 from where it is seen that the value of H increases with $Z_p Z_T$ and it is lower for smaller value of s_{inj} . In the present work we adopt the linear expression for s_{inj} , Eq. (5), as the input to the calculation.

As far as survival probability (P_{Surv}) is concerned, in cold fusion reactions when only one neutron is emitted from the compound nucleus, P_{Surv} is the product of probability to emit a neutron in the first stage of de-excitation process and the probability $P_{<}$ that the excitation energy (after the emission of neutron) is less than the threshold for second chance fission or second neutron emission (which ever is lower) [18,21]:

$$P_{Surv} = \frac{\Gamma_n}{\Gamma_n + \Gamma_f} P_{<}, \quad (6)$$

where Γ_n and Γ_f are the partial decay widths for first chance neutron emission and fission, respectively. The neutron width is calculated by using the Weisskopf formula [21],

$$\Gamma_n = \frac{g_n m_n \sigma_n}{\pi^2 \hbar^2 \rho_A(E_A^*)} \int_0^{E_{A-1}^{* \max}} \rho_{A-1}(E_{A-1}^{* \max} - \epsilon_n) \epsilon_n d\epsilon_n, \quad (7)$$

where the product of the kinetic energy of the emitted neutron ϵ_n and the level density of the daughter nucleus (ρ_{A-1}) is integrated over ϵ_n from 0 to a maximum possible energy $E_{A-1}^{* \max} =$

$E_A^* - S_n^A - E_{(A-1)}^{\text{pair}}$, where E_A^* is the excitation energy of the parent nucleus, S_n^A is the neutron separation energy of the parent nucleus, and $E_{(A-1)}^{\text{pair}}$ is the pairing energy in the daughter nucleus. In Eq. 7, $g_n = 2$ is the neutron spin degeneracy, m_n is the neutron mass, $\sigma_n \approx \pi r_0^2 A^{2/3}$ with $r_0 = 1.45$ fm stands for the inverse cross section for the neutron evaporation, and $\rho_A(E_A^*)$ is the level density of the parent nucleus at the initial excitation energy E_A^* .

The fission width is given by the transition state theory [21],

$$\Gamma_f = \frac{1}{2\pi\rho_A(E_A^*)} \int_0^{E_{A,sd}^{*\max}} \rho_{A,sd}(E_{A,sd}^{*\max} - \epsilon_f) d\epsilon_f, \quad (8)$$

where ϵ_f is the kinetic energy in the fission degree of freedom, $\rho_{A,sd}$ is the level density of the fissioning nucleus of mass A at the saddle point. The maximum possible thermal excitation energy at the saddle point is $E_{A,sd}^{*\max} = E_A^* - B_f - E_A^{\text{pair}}$, where B_f and E_A^{pair} are the fission barrier and the pairing energy of the fissioning nucleus. The factor $P_<$ in Eq. (6) is the probability that evaporation of a neutron will bring the final nucleus $(A - 1)$ below the threshold for the second chance fission, $E_{A-1}^{*\text{thr}}(f) = B_f^{A-1}$, or the threshold for emission of a second neutron, $E_{A-1}^{*\text{thr}}(n) = S_n^{A-1}$, which ever is lower. Therefore,

$$P_< = \frac{\int_{\epsilon_{\text{thr}}}^{E_{A-1}^{*\max}} \rho_{A-1}(E_{A-1}^{*\max} - \epsilon_n) \epsilon_n d\epsilon_n}{\int_0^{E_{A-1}^{*\max}} \rho_{A-1}(E_{A-1}^{*\max} - \epsilon_n) \epsilon_n d\epsilon_n}, \quad (9)$$

where the threshold value of the variable ϵ_n is, $\epsilon_{\text{thr}} = E_{A-1}^{*\max} - E_{A-1}^{*\text{thr}}$ or $\epsilon_{\text{thr}} = 0$ if $E_{A-1}^{*\max} - E_{A-1}^{*\text{thr}} \leq 0$. Here, $E_{A-1}^{*\text{thr}} = \min[E_{A-1}^{*\text{thr}}(f), E_{A-1}^{*\text{thr}}(n)]$.

3.1. Level densities, shell effects, and fission barriers

The level density for a nucleus of mass number A , and excitation energy E^* is taken from Fermi-gas model formalism [18,21],

$$\rho(U) = \exp(2\sqrt{aU}), \quad (10)$$

where U is the effective excitation energy corrected for its pairing energy, E^{pair} , $U = E^* - E^{\text{pair}}$, where, $E^{\text{pair}} = 21/\sqrt{A}$ MeV, $10.5/\sqrt{A}$ MeV, and 0 for even-even, odd, and odd-odd nuclei, respectively. We used Ignatyuk's prescription for the level density parameter a , which is widely used in the phenomenological descriptions of the nuclear level density [21,39]:

$$a = \tilde{a} \left\{ 1 + \frac{E_{\text{shell}}}{U} [1 - \exp(-\gamma U)] \right\}, \quad (11)$$

where \tilde{a} is the asymptotic value of the level-density parameter and γ is the shell damping parameter for which we have used the value 0.054 MeV^{-1} [21,39]. The ground state shell correction energy $E_{\text{shell}(g.s.)}$ is taken from Möller et al. [34], while for the saddle point no shell effect is assumed, $E_{\text{shell}(saddle)} = 0$. The shape dependent asymptotic value of the level-density parameter, \tilde{a} , has been used from Reisdorf's formalism [21,40]. The fission barrier height (B_f^A) including the washing out of the shell effects with effective excitation energy (U), is given as [41]:

$$B_f^A = B_f^{\text{LD},A} + B_f^{\text{mic},A} \exp(-U/E_D^A), \quad (12)$$

where $B^{\text{LD},A}$ is the liquid drop part of the fission barrier which is calculated using the improved version of algebraic equations [21], as discussed earlier. The liquid drop part of the fission barrier for the present reactions involving rare earth nuclei is essentially

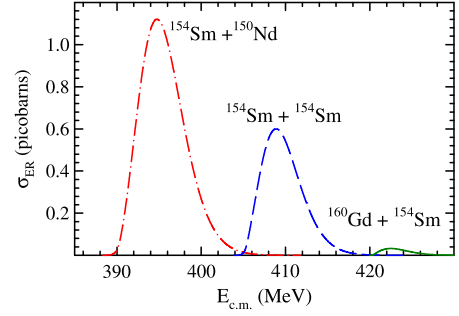


Fig. 4. (Color online.) Excitation function for $1n$ channel evaporation residue cross section calculated within the framework of the FBD model for the present reactions involving rare-earth nuclei. For $^{160}\text{Gd} + ^{154}\text{Sm}$ reaction, $B_f^A = B_f^{A-1} = 1.0$ MeV.

zero, it is the only microscopic part which gives stability against the fission. The microscopic part of the fission barrier, $B^{\text{mic},A} = -E_{\text{shell}(g.s.)}^A$, where $E_{\text{shell}(g.s.)}^A$ is the shell correction energy in the ground state, taken from Ref. [34]. There are several prescriptions for the damping parameter E_D^A , and here it is taken as [42]:

$$E_D^A = \frac{5.48A^{1/3}}{1 + 1.3A^{-1/3}}. \quad (13)$$

It should be noted here that the excitation and neutron separation energies of a given nucleus are evaluated using the mass tables of Möller et al. [34] (when it is not available experimentally).

3.2. Excitation functions and cross sections

Using the model outlined above, it is seen that for all the GSI data, the peak cross sections and the peak energies of the excitation functions are consistent with experimental values. For the present systems of $^{154}\text{Sm} + ^{150}\text{Nd}$ and $^{154}\text{Sm} + ^{154}\text{Sm}$ reactions, the excitation functions are shown in Fig. 4. The peak cross sections are obtained as 1.1 and 0.6 picobarns, respectively for these two systems. For $^{160}\text{Gd} + ^{154}\text{Sm}$ reaction, the B_f^A as well as B_f^{A-1} are found to be negative from the predictions of Möller et al. [34] which is unphysical. However, it is found by different authors [43, 44] that the fission barriers for $Z \geq 120$ systems vary widely between 2 to 8 MeV. For the sake of present calculations we have taken a nominal value of $B_f^A = B_f^{A-1} = 1.0$ MeV for $^{160}\text{Gd} + ^{154}\text{Sm}$ reaction, for which the excitation function is also shown in Fig. 4. Thus, it may be noted that the present reactions involving rare earth nuclei seem to be quite encouraging, showing peak cross sections of around 1 picobarn for $Z = 122$ and 124 systems.

Present work suggests it to be definitely worth for experimental investigations using rare-earth nuclear collisions. Also it points out to the necessity for carrying out full microscopic calculations to understand the fusion mechanism for these heavy deformed systems.

4. Summary

In the present work, we have made a case for the use of rare-earth projectile and target nuclei to produce super-heavy nuclei in the range of $Z \sim 120$ and above using cold fusion reactions. The advantages offered by these near-symmetric collisions have been outlined. The cross sections for production of the super-heavy nuclei in these collisions have been estimated within the framework of the Fusion by Diffusion model with empirically derived parameter values and are seen to be quite encouraging. These reactions offer an alternate attractive route to the conventional near-symmetric 'cold fusion' and highly asymmetric 'hot fusion' reaction

channels for synthesis of super-heavy nuclei with $Z > 120$. It is, however, necessary to carry out experiments to explore these possibilities of using rare-earth nuclei for production of super-heavy elements.

Acknowledgements

Authors are thankful to Dr. S.S. Kapoor and Dr. V.M. Datar for many useful discussions.

References

- [1] W.D. Myers, W.J. Swiatecki, Nucl. Phys. 81 (1966) 1.
- [2] U. Mosel, W. Greiner, Z. Phys. 217 (1968) 256;
U. Mosel, W. Greiner, Z. Phys. 222 (1969) 261.
- [3] S.G. Nilsson, et al., Nucl. Phys. A 115 (1968) 545;
S.G. Nilsson, S.G. Thompson, C.F. Tsang, Phys. Lett. B 28 (1969) 458.
- [4] S.G. Nilsson, et al., Nucl. Phys. A 131 (1969) 1.
- [5] J.R. Nix, Annu. Rev. Nucl. Sci. 22 (1972) 65.
- [6] Yu.Ts. Oganessian, et al., Nature 400 (1999) 242.
- [7] Yu.Ts. Oganessian, et al., Phys. Rev. Lett. 83 (1999) 3154.
- [8] Yu.Ts. Oganessian, et al., Phys. Rev. C 69 (2004) 054607.
- [9] Yu.Ts. Oganessian, et al., Phys. Rev. C 72 (2005) 034611.
- [10] Yu.Ts. Oganessian, et al., Phys. Rev. C 74 (2006) 044602.
- [11] Yu.Ts. Oganessian, et al., Phys. Rev. Lett. 104 (2010) 142502.
- [12] L. Stavsetra, K.E. Gregorich, J. Dvorak, P.A. Ellison, I. Dragojevic, M.A. Garcia, H. Nitsche, Phys. Rev. Lett. 103 (2009) 132502.
- [13] S. Hofmann, Rep. Prog. Phys. 61 (1998) 639.
- [14] S. Hofmann, G. Münzenberg, Rev. Mod. Phys. 72 (2000) 733.
- [15] S. Hofmann, et al., Nucl. Phys. A 734 (2004) 93.
- [16] K. Morita, et al., J. Phys. Soc. Jpn. 81 (2012) 103201.
- [17] W.J. Swiatecki, K. Siwek-Wilczynska, J. Wilczynski, Int. J. Mod. Phys. E 13 (2004) 261.
- [18] W.J. Swiatecki, K. Siwek-Wilczynska, J. Wilczynski, Phys. Rev. C 71 (2005) 014602.
- [19] K. Siwek-Wilczynska, I. Skwira-Chalot, J. Wilczynski, Int. J. Mod. Phys. E 16 (2007) 483.
- [20] V. Zagrebaev, W. Greiner, Phys. Rev. C 78 (2008) 034610.
- [21] T. Cap, K. Siwek-Wilczynska, J. Wilczynski, Phys. Rev. C 83 (2011) 054602.
- [22] Yu-Jie Liang, M. Zhu, Zu-Hua Liu, Wen-Zhong Wang, Phys. Rev. C 86 (2012) 037602.
- [23] R. Smolanczuk, Phys. Rev. C 63 (2001) 044607.
- [24] V.Yu. Denisov, Prog. Part. Nucl. Phys. 46 (2001) 303.
- [25] V. Zagrebaev, W. Greiner, Nucl. Phys. A 834 (2010) 366c.
- [26] A. Iwamoto, P. Möller, J.R. Nix, H. Sagawa, Nucl. Phys. A 596 (1996) 329.
- [27] W. Nörenberg, in: Proc. Int. Workshop on Heavy-Ion Fusion, Padua, Italy, 1994.
- [28] W. Nörenberg, GSI Nachrichten 10-94 (1994) 13.
- [29] Y. Aritomo, T. Wada, M. Ohta, Y. Abe, Phys. Rev. C 55 (1997) R1011.
- [30] W. Greiner, J. Phys. Conf. Ser. 337 (2012) 012002.
- [31] S. Hofmann, Prog. Part. Nucl. Phys. 46 (2001) 293.
- [32] D. Ackermann, Eur. Phys. J. A 25 (2005) 577.
- [33] Yu.Ts. Oganessian, et al., Phys. Rev. C 79 (2009) 024608.
- [34] P. Möller, J.R. Nix, W.D. Myers, W.J. Swiatecki, At. Data Nucl. Data Tables 59 (1995) 185.
- [35] Nuclear reaction video project, <http://nrv.jinr.ru/nrv>.
- [36] W.J. Swiatecki, Phys. Scr. 24 (1981) 113.
- [37] S. Bjørnholm, W.J. Swiatecki, Nucl. Phys. A 391 (1982) 471.
- [38] C.Y. Wong, Phys. Rev. Lett. 31 (1973) 766.
- [39] Y.K. Gupta, et al., Phys. Rev. C 78 (2008) 054609.
- [40] W. Reisdorf, Z. Phys. A 300 (1981) 227.
- [41] W. Li, Z. Wang, H. Xu, et al., Chin. Phys. Lett. 21 (2004) 636.
- [42] A.V. Ignatyuk, et al., Sov. J. Nucl. Phys. 21 (1975) 612.
- [43] H. Koura, J. Nucl. Radiochem. Sci. 3 (2002) 201.
- [44] J.A. Sheikh, W. Nazarewicz, J.C. Pei, Phys. Rev. C 80 (2009) 011302(R).